

See discussions, stats, and author profiles for this publication at: <https://www.researchgate.net/publication/232693195>

# The Vertical Distribution of Runoff and its Suspended Load in Lake Malawi

Article in *Journal of Great Lakes Research* · January 2009

DOI: 10.3394/0380-1330(2007)33[449:TVDORA]2.0.CO;2

---

CITATIONS

11

---

READS

55

3 authors, including:



[Greg Mccullough](#)

University of Manitoba

18 PUBLICATIONS 304 CITATIONS

[SEE PROFILE](#)



[Paul Mason Cooley](#)

North/South Consultants Inc.

12 PUBLICATIONS 61 CITATIONS

[SEE PROFILE](#)

Some of the authors of this publication are also working on these related projects:



Mitigation and effectiveness monitoring of hydroelectric dam operations on recruitment of juvenile Lake Sturgeon [View project](#)

All content following this page was uploaded by [Greg Mccullough](#) on 02 January 2014.

The user has requested enhancement of the downloaded file. All in-text references [underlined in blue](#) are added to the original document and are linked to publications on ResearchGate, letting you access and read them immediately.

## The Vertical Distribution of Runoff and its Suspended Load in Lake Malawi

Greg K. McCullough\*, David Barber, and Paul M. Cooley

Centre for Earth Observations Science  
Department of Environment and Geography  
University of Manitoba  
Winnipeg R3T 2N2

**ABSTRACT.** Lake Malawi, in south-eastern Africa, is subject to increasing loading of suspended solids caused by land use pressure in its watershed. Whether this load is transported into the lake as overflow, interflow or deep underflow determines to a large extent its effect on the lake ecosystem. In this paper, vertical distributions of suspended solids in the Linthipe River delta region of the lake are described from multiple surveys during two rainy seasons. These data are supplemented by data from a single survey near four northern rivers also tributary to the lake. Profiles of temperature, conductance, and suspended solids concentrations (SSC, estimated from optical backscatter and beam transmission) are used to identify fluvial intrusions into the water column. Most inflow plunged to the seasonal metalimnion where it spread along high density gradients as interflow. While SSC in surface plumes rarely exceeded  $10 \text{ g m}^{-3}$ , and in intrusions in the lower metalimnion was rarely greater than  $1 \text{ g m}^{-3}$ , concentrations up to  $420 \text{ g m}^{-3}$  were recorded in interflow near the thermocline. Although storm runoff density often exceeded 100 m depth-equivalence in the lake, underflow density was reduced to metalimnion-equivalence (30–50 m depth) within a few 100s of meters of the river mouth. We attribute bottom-attached turbid layers, and the few unattached turbid layers in the lower metalimnion, all with positive conductance anomalies, to sediment resuspension and not to runoff. We conclude that the upper metalimnion is the prevailing pathway carrying watershed runoff horizontally throughout Lake Malawi.

**INDEX WORDS:** Delta processes, mixing, sediment transport, hyperycnal flow, interflow, Lake Malawi.

### INTRODUCTION

The fishes of Lake Malawi (known as Lake Nyasa in Tanzania, and Lake Niassa in Mozambique) are a major source of protein for the people of Malawi and because of their beauty and diversity, a significant component of the tourist economy. Increasing nutrient and sediment yields associated with development in the watershed (Hecky *et al.* 2003) may have an adverse impact on this valuable resource. Several recent studies have documented reductions in benthic invertebrate abundance (Amin and Barton 2003), fish condition (Duponchelle *et al.* 2000) and species richness (Sululu 2000) associated with seasonal sediment discharge into Lake Malawi. Hecky *et al.* (2003) showed that 80–90% of major nutrients in stream flow into Lake Malawi is transported in the sus-

pended load. Guildford *et al.* (1998) showed that increasing loading of phosphorous in particular may be expected to favor nitrogen fixing, filamentous cyanobacteria, including species toxic to both fish fauna and humans.

Some runoff into Lake Malawi sinks to the metalimnion (Halfman and Scholz 1993) and it has been argued that hyperycnal flow may at times pass below the chemocline (Johnson *et al.* 1995, Kingdon *et al.* 1998, Vollmer *et al.* 2005). However, although underflow can persist to the bottom in stratified temperate-latitude lakes (*e.g.*, Lambert *et al.* 1976, Wüest *et al.* 1988), this has not been demonstrated for deep tropical lakes. The biological impact of increased inputs of suspended solids varies with the depth to which the load is delivered. Light attenuation, which would tend to reduce productivity, is maximized where sediment-laden runoff spreads buoyantly. Attenuation is negligible

\*Corresponding author. E-mail: GregMcCullough@cc.umanitoba.ca

where runoff plunges below the euphotic zone, unless particulates in deep interflow layers are mixed back to the surface. In the short term, the latter case may be optimal for primary production, in that the dissolved nutrient load is returned to the euphotic zone even as light attenuation is reduced because some of the larger/more dense particulates will have settled out. In the longer term, dissolved nutrients carried to any depth in Lake Malawi are eventually returned to the surface by vertical mixing (Bootsma and Hecky 1993). In anoxic water, as below 250 m in Lake Malawi, particle-bound iron and with it, sorbed phosphorous are released into solution (Hecky *et al.* 1996). Consequently, hyperpycnal flow into the monimolimnion could actually increase the fraction of biologically available phosphorous and iron in the total load delivered by runoff, at least relative to any process that resulted in losses of suspended particulates by sedimentation above the chemocline.

In a companion paper in this issue, McCullough and Barber (2007) discuss the degree and spatial extent of light attenuation by turbid surface plumes developed in Lake Malawi near the mouth of the Linthipe River. In this paper, we use data from CTD (conductivity, temperature, and depth profiler, in this case with additional sensors allowing estimation of suspended solids concentration) surveys completed over the course of two rainy seasons to develop a statistical summary of vertical distributions of suspended solids in Lake Malawi near the mouth of the Linthipe River. We show how these distributions result from a particular history of river-lake density relationships over each rainy season. Using CTD casts recorded near the mouths of northern tributary rivers, we examine the applicability of our results to the whole lake. Finally, we argue that the metalimnion is the prevailing pathway carrying watershed runoff horizontally throughout Lake Malawi, and that deeper sinking of runoff must be an infrequent event at best.

### STUDY REGION

Lake Malawi is the southernmost of the East African Rift Lakes. It is 560 km long, 40–70 km wide, and 22,490 km<sup>2</sup> in area, with a terrestrial watershed of 75,300 km<sup>2</sup> (Spigel and Coulter 1996) (Fig. 1). It is a stratified lake, with a seasonal thermocline that develops in late November or December at 20–50 m depth and that is progressively eroded in a windy season that begins in April or May, until the lake is mixed to 100–150 m depth by

July or August (Patterson and Kanchinjika 1995). Water deeper than 200–250 m is perennially homothermal and anoxic (Gonfiantini *et al.* 1979, Vollmer *et al.* 2002) but not wholly isolated from upper layers. Estimates of exchange rates between the upper mixed layer and the monimolimnion range from 5–6% of its volume per year (Vollmer *et al.* 2002) up to 20% y<sup>-1</sup> (Gonfiantini *et al.* 1979) and higher.

The site of this study is a semicircular region around the mouth of the Linthipe River in southern Lake Malawi (Fig. 1). The Linthipe River drains an 8,560 km<sup>2</sup> watershed and is the fourth largest tributary to Lake Malawi. Over 90% of its discharge occurs in the rainy season months of December–April (DOW 1986). At its mouth, it has formed a small Gilbert-type sand delta with a sub-aqueous distributary plain bounded by intermittently sub-aqueous/sub-aerial shoals and a steep foreset face. Hyperpycnal flow down the delta front is mostly constrained to south-eastward path by a subaqueous ridge underlying the Maleri Island chain (Fig. 1).

### METHODS

Data for this study were collected during the 1998 and 1999 rainy seasons, mostly in the form of water column profiles along up to five transects radiating outward into Lake Malawi from near the mouth of the Linthipe River. We recorded 534 vertical water column profiles of pressure, temperature (*T*), conductivity (corrected to specific conductance at 20°C = *K*), and optical backscatter using a Richard Brancker Research (RBR) Limited XP-400 CTD. Another 114 profiles of pressure, *T*, *K* and beam transmission were recorded with a Sea-Bird Electronics Inc. SeaCat SBE 19-01 CTD. Linthipe River water was sampled and RBR CTD casts were recorded at a point in fast-flowing water near the center of the channel 200–300 m upstream of the lake. CTD data were averaged at 1 m intervals prior to further processing. River water samples were depth integrated to about 10 cm from the bottom, in a channel typically 0.5–1.5 m deep. All sensors on the RBR CTD were recalibrated by the manufacturer prior to each field season. Sensors on the SBE CTD were recalibrated by the manufacturer in 1996. The SBE CTD beam transmissometer was recalibrated in the field in December 1977 and March 1999. Station locations were determined using a Trimble® Scout Global Positioning Systems (GPS) unit. GPS data were not differentially corrected.

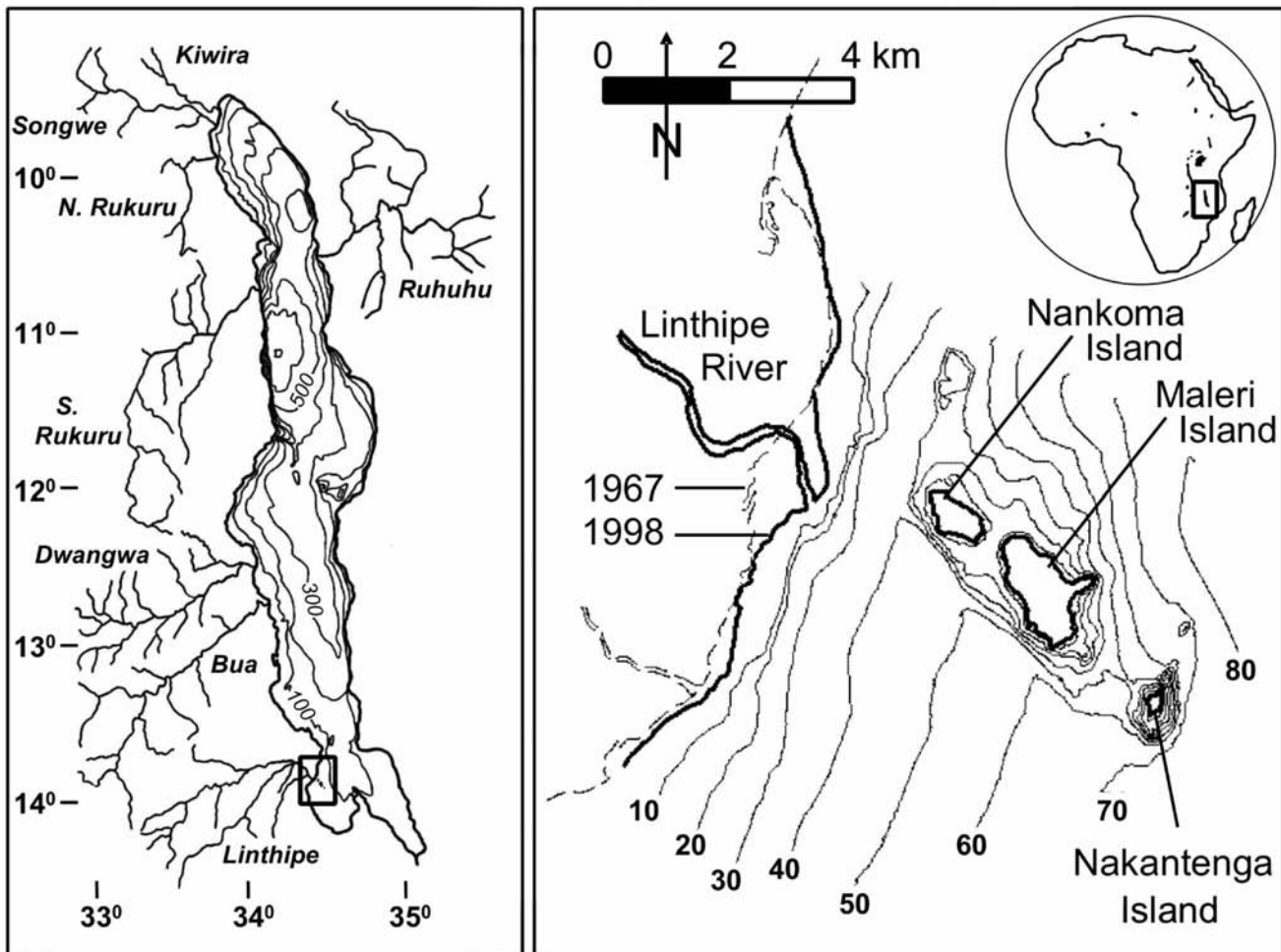


**FIG. 1.** Lake Malawi, showing major tributary rivers (left), and the Linthipe River delta region (right). The 1967 shoreline is from a 1:50000 topographic survey map based on 1967 aerial photography. The 1998 shoreline was determined using a geocorrected Landsat Thematic Mapper image. Whole-lake bathymetry is after Johnson et al. (1995). Delta region bathymetry was prepared from sonar data recorded in January and February, 1999 (Cooley 2004). Isobath units are meters.

Accuracy of individual location determinations is of the order of  $\pm 100$  m.

Sea-Bird Electronics Inc. claimed an accuracy of  $0.001^{\circ}\text{C}$  for  $T$  and  $3.7 \mu\text{S cm}^{-1}$  for  $K$  (95% confidence). We inferred from paired RBR CTD and SBE CTD data that the RBR CTD returned  $T$  and  $K$  with accuracies of  $0.01^{\circ}\text{C}$  and  $4.5 \mu\text{S cm}^{-1}$  respectively (95% confidence). Linthipe River temperature ( $T_{LR}$ ) was recorded using Onset Computer Corporation Hobo™ XT and StowAway™ temperature loggers tethered at approximately 0.5 m depth in fast moving water, approximately 150 m upstream of the river mouth. To remove possible systematic error between instruments, the Onset data were adjusted to minimize the mean difference with

RBR CTD mean water column temperatures recorded near the center of the channel near the Onset station. The larger of standard deviations of differences remaining between the adjusted differences,  $0.11^{\circ}\text{C}$  (in 1998 with  $n = 6$ , and  $0.07^{\circ}\text{C}$  in 1999 with  $n = 9$ ) serves as a conservative estimate of uncertainty in relative river and lake temperature.

Suspended solids concentrations (SSC) in RBR CTD casts were determined by polynomial regression on optical backscatter recorded using a D&A Instruments OBS-3B instrument mounted on the RBR CTD, and in SBE CTD casts by linear regression on the beam transmission measured with a 0.25 m Sea Tech Inc. transmissometer. SSC data for

validation of these empirical relationships were determined by filtration using Whatman® GF/C filters with a nominal pore size of 1.2 µm. For river water, with relatively high SSC, the coefficients of variation of triplicate SSC determinations averaged 7.9%. (n = 9). For paired lake water samples where  $SSC < 10 \text{ g m}^{-3}$ , the coefficients of variation from the means averaged 15% (n = 31). Optical backscatter predicted SSC at high concentrations with a root mean square error (RMSE) of  $144 \text{ g m}^{-3}$  [for  $SSC > 520 \text{ g m}^{-3}$ , *i.e.*, most river observations,  $P = 0.000$ ,  $r^2 = 0.99$ , n = 13]. A single polynomial calculated on the whole data set does not accurately depict the relationship at low SSC. Using a separate equation, optical backscatter predicted lower concentrations with an RMSE of  $2.0 \text{ g m}^{-3}$  [for  $SSC < 230 \text{ g m}^{-3}$ , *i.e.*, most lake observations,  $P = 0.000$ ,  $r^2 = 0.99$ , n = 39]. Beam transmission predicted SSC with a standard error of  $1.4 \text{ g m}^{-3}$  ( $P = 0.000$ ,  $r^2 = 0.97$ , n = 35). Transmission was reduced to near-zero at  $SSC > 40 \text{ g m}^{-3}$ . Calculated  $SSC < 0.01 \text{ g m}^{-3}$  is treated as “below detection.”

Density of the liquid fraction of river and lake water was calculated from temperature and salinity using the equations of state of Chen and Millero (1986) with salinity estimated as a function of  $T$ , pressure and  $K$  data using equations determined by Wüest *et al.* (1996) for Lake Malawi. For the purpose of estimating the bulk density, the suspended fraction was treated as a mixture of mineral and organic matter, with the organic fraction predicted as a function of SSC. Loss on ignition ( $LOI = \% \text{ organic matter}$ ) was determined for 75 river and lake water samples.  $LOI$  is strongly predicted by a polynomial regression [ $P = 0.000$ ,  $r^2 = 0.89$ , n = 75 (McCullough 2006)]. For  $SSC > 5 \text{ g m}^{-3}$ , SSC predicts  $LOI$  with RMSE = 2.8% (n = 46). The error term is larger at low SSC (for  $SSC < 5 \text{ g m}^{-3}$  RMSE = 16%, n = 29) but such low SSC makes a non-significant contribution to the density variability in the lake. Dry densities of  $2,650 \text{ kg m}^{-3}$  and  $1,800 \text{ kg m}^{-3}$  were assumed for the mineral and organic fraction of the river load respectively (McCullough 2006).

Combining uncertainty in  $T$  and  $K$ , in SSC prediction by optical instruments, and in mineral and organic composition and density, a conservative 95% confidence interval for bulk density is  $\pm 0.02 \text{ kg m}^{-3}$  for  $SSC < 530 \text{ g m}^{-3}$  (McCullough 2006). At the highest SSC measured lakeward of the 20 m isobath,  $1,440 \text{ g m}^{-3}$ , the 95% confidence interval is  $\pm 0.5 \text{ kg m}^{-3}$ . In context,  $0.5 \text{ kg m}^{-3}$  was half the typical density range through the upper 70 m of the

water column during the 1997/98 and 1998/99 rainy seasons.

The suspended solids load within a 7 km radius of the Linthipe River was mapped from survey data on 3 days after a large storm runoff event. SSC ( $\text{g m}^{-3}$ ) was summed through 10 m intervals in each profile to yield the suspended solids load in each 10 m layer of the water column ( $SSL_{10}$ ,  $\text{g m}^{-2}/10\text{m}$ ).  $SSL_{10}$  was determined for 1 km grid cells as the inverse-distance-squared weighted mean of  $SSL_{10}$  in nearest-neighbor profiles in each surrounding octant, and then grid cells were added to estimate the load in semi-circular regions around the river mouth.

Through the rainy season, in most CTD casts we encountered relatively high thermal gradients ( $0.1\text{--}0.5^\circ\text{C m}^{-1}$ ) in a layer of varying thickness between depths of 20–70 m. A sharp break in  $K$  profiles at the lower depth indicated that surface water occasionally mixed as deeply as, but rarely more than 60–70 m in either of the two rainy seasons. This transition region falls entirely within the epilimnion as defined for Lake Malawi (0–105 m) by Gonfiantini *et al.* (1979) and Vollmer *et al.* (2002), with the metalimnion falling below 105 m. However, in this study we use the term metalimnion to refer to the shallower transitional layer that we observed during the rainy seasons, specifically defining it by a thermal gradient  $> 0.05^\circ\text{C m}^{-1}$ . We define the thermocline as the depth of the maximum water column temperature gradient determined from profile data smoothed by a 3 m moving average, excluding the upper 5 m of the water column in order to exclude shallow diurnal gradients. The thermocline usually fell in the upper 10 m of the metalimnion. Regional daily mean thermocline depths are calculated from data in CTD casts  $> 7 \text{ km}$  from the river, *i.e.*, beyond local effects of plunging cool river water.

Linthipe River discharge data were supplied by the Malawi Water Department.

## RESULTS

### Linthipe River Discharge, Thermal Regime, and Sediment Load

December–April mean discharge in 1997/98 and 1998/99 was  $138$  and  $241 \text{ m}^3 \text{ s}^{-1}$ , *i.e.*, 1.6 times and 2.8 times the long term mean of  $86 \text{ m}^3 \text{ s}^{-1}$  (Kidd 1983). Suspended solids concentration ( $SSC_{LR}$ ) was determined 17 times between 15 January–10 March 1998 and 14 times between 22 January–4 April 1999 (Fig. 2). It averaged  $1,280 \text{ g m}^{-3}$  in 1998 and  $1,952 \text{ g m}^{-3}$  in 1999, and ranged from 85–4,385

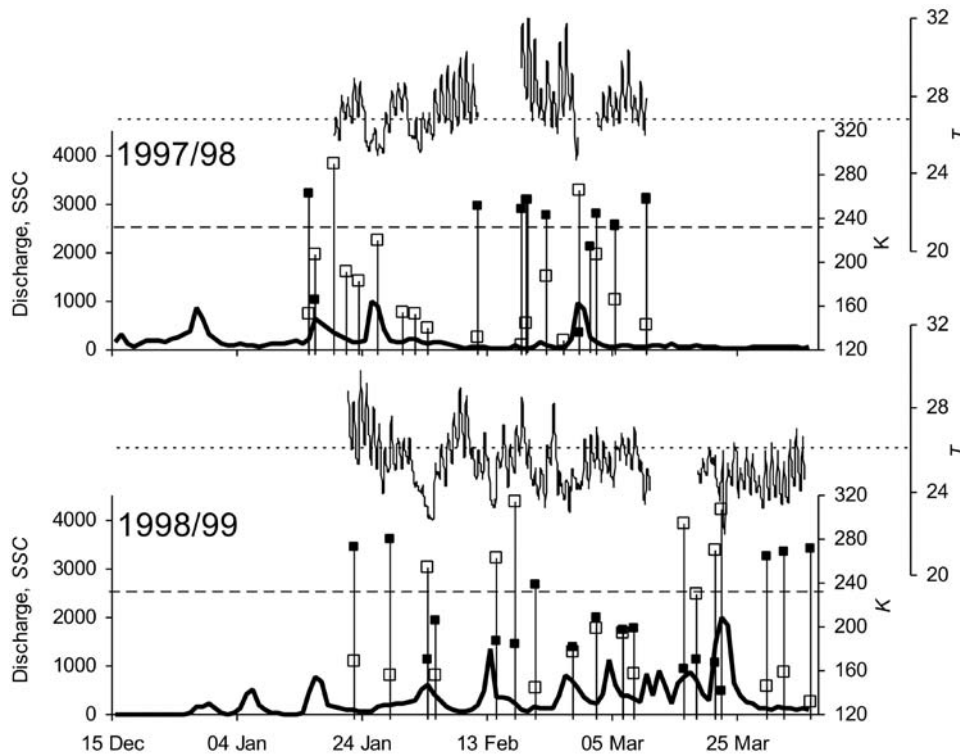


**FIG. 2.** Linthipe River daily mean discharge (heavy line,  $\text{m}^3 \text{s}^{-1}$ ),  $\text{SSC}_{LR}$  ( $\square$ ,  $\text{g m}^{-3}$ ),  $T_{LR}$  (light line, hourly mean,  $^{\circ}\text{C}$ ) and  $K_{LR}$  ( $\blacksquare$ ,  $\mu\text{S cm}^{-1}$ ). Horizontal lines indicate the rainy season mean thermocline temperature (dotted line) and the mean ambient epilimnion  $K$  (dashed line).

$\text{g m}^{-3}$  through the two rainy seasons. Correlation between natural logarithms of daily suspended solids load and daily discharge ( $r^2 = 0.88$ ,  $n = 31$ ) was used to estimate total December–April rainy season loads of 2.9 and 7.3 Tg (3.4 and 8.5  $\text{Mg}\cdot\text{ha}^{-1}$ ) in 1997/98 and 1998/99 respectively.

The higher discharge in 1999 was associated with lower mean  $T_{LR}$ , 25.5 $^{\circ}\text{C}$  in 1999 compared to 27.5 $^{\circ}\text{C}$  in 1998 for the same period, 22 January–10 March, in each rainy season. Diurnal variation was typically 2–3 $^{\circ}\text{C}$  and as large as 5 $^{\circ}\text{C}$ . The upper mixed layer of the lake was also slightly cooler in 1999 compared to 1998. In 1999, the upper 10 m cooled slightly from 28.1 $^{\circ}\text{C}$  in January to 27.8 $^{\circ}\text{C}$  by March. Through the same period in 1998, it warmed from 28.7 $^{\circ}\text{C}$  to 29.2 $^{\circ}\text{C}$ . Throughout both rainy seasons—excepting only a few days in mid-February 1998—the upper mixed layer was almost always warmer than the daily mean  $T_{LR}$ , even under low flow conditions, although the difference was generally greater in the 1999 rainy season.

The thermocline tended to be deeper and cooler in 1999 than in 1998. In 1998, it averaged 38 m,

and ranged from 25–50 m depth. In 1999 it averaged 44 m and ranged from 35–55 m depth. The mean  $T$  at the thermocline was 26.8 $^{\circ}\text{C}$  in 1998, compared to 26.1 $^{\circ}\text{C}$  in 1999. Nonetheless, because the inter-annual differences in  $T_{LR}$  were greater, the river was cooler than thermocline depth more frequently in 1999 than in 1998—more than three-quarters of the time in 1999, but only about half of the time in 1998 (Fig. 2).

Inter-relationships between discharge and the three parameters relating to density are shown in Figure 3.  $\text{SSC}$  in the river ( $\text{SSC}_{LR}$ ) was positively correlated with discharge in each year, with regressions not significantly different between years, ( $P = 0.000$ ,  $r^2 = 0.51$ ,  $n = 28$  for the pooled data).  $T_{LR}$  and conductance in the river ( $K_{LR}$ ) were each inversely correlated with river discharge ( $P < 0.003$ ) in each year, but regressions were significantly different between years. However, the interaction of river density and lake density structure is better investigated by a parameter relating  $T_{LR}$  and the temperature of the epilimnion. With the temperature at 10 m ( $T_{LM10}$ ) representing the latter, the parameter

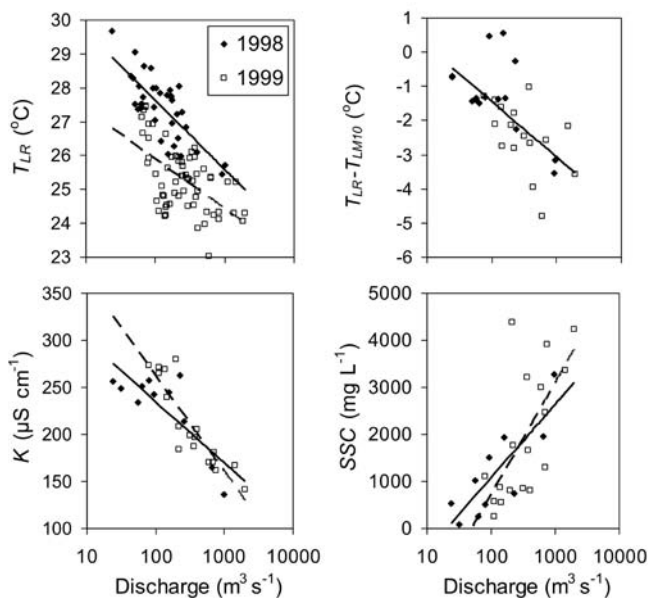


**FIG. 3.** Linthipe River daily mean  $T_{LR}$  (upper left),  $T_{LR} - T_{10m}$  (upper right),  $K_{LR}$  (lower left) and  $SSC_{LR}$  (lower right) plotted against daily mean discharge.  $T_{LR} - T_{10m}$  is the daily mean lake temperature at 10 m depth (averaged from CTD casts, excluding casts < 6 km from the river) subtracted from the daily mean temperature in the river. The trend line shown for  $T_{LR} - T_{10m}$  vs. discharge is for pooled years; others are for annual subsets (solid = 1998, dashed = 1999).

$T_{LR} - T_{LM10}$  can serve to represent relative river and epilimnion temperature.  $T_{LR} - T_{LM10}$  was correlated with discharge in each year, and the regressions are not significantly different between years ( $P = 0.000$ ,  $r^2 = 0.42$ ,  $n = 33$  for the pooled data).

#### Linthipe River Density and Lake Malawi Density Structure

Density structure of the water column is shown through time in Figure 4, in which bulk densities are interpolated between values calculated from  $T$ , salinity derived from  $K$ , and  $SSC$  (as observed in casts > 7 km from the river mouth).  $SSC$  contributed at most  $0.07 \text{ kg m}^{-3}$  to bulk density at any point in the water column at these offshore stations. Temperature contributed  $2 \text{ kg m}^{-3}$  to the density range of the Linthipe River over each of the two field seasons, and as much as  $1.6 \text{ kg m}^{-3}$  diurnally.  $K$  contributed negligibly to density variability. However, in 1998  $SSC_{LR}$  contributed an additional

$2 \text{ kg m}^{-3}$  ( $100 < SSC_{LR} < 3,360 \text{ g m}^{-3}$ ,  $n = 19$ ) to density variability, and in 1999 over  $3 \text{ kg m}^{-3}$  ( $250 < SSC_{LR} < 5,320 \text{ g m}^{-3}$ ,  $n = 17$ ). Over the 1999 rainy season, the density range of inflow density exceeded the density range of the lake. However, dilution and sedimentation dramatically reduced the river-lake density difference within a few 100s of meters of the river mouth (McCullough 2006). CTD data near the mouth of the Linthipe River show anomalies in  $T$ ,  $K$ , and  $SSC$  which indicate layers of mixed river and lake water in underflow and interflow, all of which become less pronounced with increasing distance from the river mouth. For example, on the day of our highest  $SSC_{LR}$  determination in the 2-year study, 17 February 1999, when river water density was  $1,000.3 \text{ kg m}^{-3}$ , the highest density observed in underflow lakeward of the 20 m isobath was  $997.5 \text{ kg m}^{-3}$ , *i.e.*, within the density range of the upper metalimnion on that day (Fig. 5). On that day,  $SSC_{LR}$  was  $5,320 \text{ g m}^{-3}$ , while the highest  $SSC$  determined in underflow just beyond the 20 m isobath was  $1,440 \text{ g m}^{-3}$ . Although  $T_{LR}$  in the hour preceding this sample had ranged from a low of  $24.5^\circ\text{C}$  in the morning to  $25.5^\circ\text{C}$  in the hour before this CTD cast, the minimum temperature in underflow at the same point was  $27.3^\circ\text{C}$ . Finally, while on this day the river was very dilute, with  $K_{LR} = 184 \mu\text{S cm}^{-1}$  compared to the  $230 \mu\text{S cm}^{-1}$  measured in ambient epilimnion lake water,  $K$  in underflow just below the 20 m isobath was depressed only to  $210 \mu\text{S cm}^{-1}$ . That is, both dilution (entrainment of warmer, lower- $SSC$  lake water) and sedimentation contributed to density reduction in the flow passing from the river into the lake. (Note that the density inversions apparent in several shallow profiles in Fig. 5 are due to both  $T$  minima and  $SSC$  maxima above the bottom of the profile; such inversions were not uncommon in CTD casts very near the river mouth, and may to be due to turbulent overturns of incompletely mixed flow.) In three deeper profiles in Figure 5,  $SSC$  peaks associated with local  $K$  minima at 45 m indicate that some flow persisted along the bottom to the thermocline, where it lifted and spread further as interflow.

Although river density exceeded lake density at 70 m depth in 4 of 13 determinations in 1998, and in 8 of 16 in 1999, we never observed this to be the case for the maximum density of the underflow beyond the 20 m isobath. On the other hand, on at least a few occasions, river water was surface-buoyant. This circumstance was rare in 1999, but may have occurred frequently the first half of Feb-

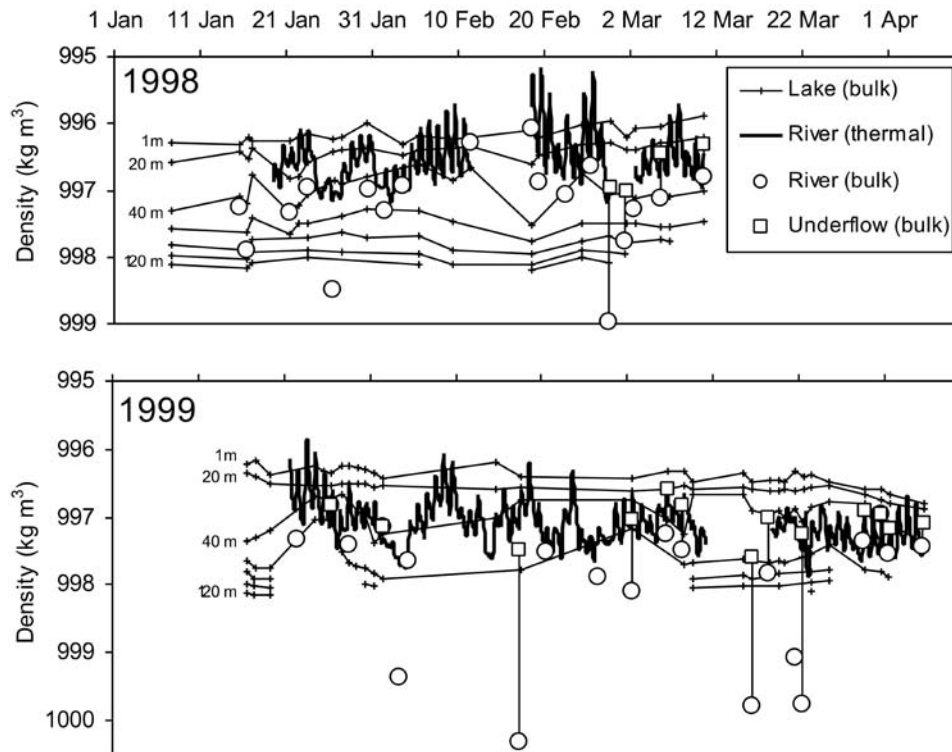


**FIG. 4.** Time series of river water density, overlaid on lake density structure. Bulk density at 1 m and from 20–120 m depth at 20 m intervals is indicated by linear interpolation between values determined from T, K, and SSC recorded in CTD casts. The thermal component of river density is indicated by heavy lines. Occasional determinations of bulk river density are shown by open squares ( $\square$ ). Occasional determinations of maximum bulk density observed in underflow lakeward of the 20 m isobath are indicated by open circles ( $\circ$ ). Vertical lines connect same-day river and maximum underflow bulk densities (only on days when data were available for both determinations) in order to highlight density losses that were observed in the transition from river to underflow.

ruary 1998, when the daytime river temperature tended to be warmer than the thermocline, and was not infrequently warmer than the surface. This period was marked by low flows and, for the most part, low SSC contributions to river water density (Fig. 4).

#### Distributions of SSC Maxima in the Delta Region

Figure 6 shows the vertical distribution of suspended solids concentration maxima ( $SSC_{max}$  = maximum SSC in a given vertical profile) in the delta region during the two rainy seasons. McCullough and Barber (2007) describe horizontal distributions of  $SSC_{max}$  separately in a companion article in this journal. SSC as high as  $4,300 \text{ g m}^{-3}$  was recorded in underflow 300 m downslope of the inlet, and as high as  $420 \text{ g m}^{-3}$  in interflow sepa-

rated from the bottom. These maxima occurred within turbid layers that were frequently many kilometres in extent and sometimes many metres in thickness (McCullough 2006). Turbid layers observed along the bottom between the river mouth and the intersection of the sediment-water interface with the thermocline were demonstrably underflow from the Linthipe River. In same-day data sets, they were typically marked by decreasing  $SSC_{max}$  with increasing distance from the river. During and soon after storm runoff events, *i.e.*, when  $SSC_{LR}$  was particularly high and  $K_{LR}$  low in the river relative to the lake, conductance minima ( $K_{min}$ ) were observed at the same or similar depths as  $SSC_{max}$ , and subsidiary SSC peaks in profiles were typically mirrored by subsidiary K anomalies. The reverse relationship (K maxima coinciding with  $SSC_{max}$ ) was observed when the river was nearer to base flow conditions, and  $K_{LR}$  was high compared to am-

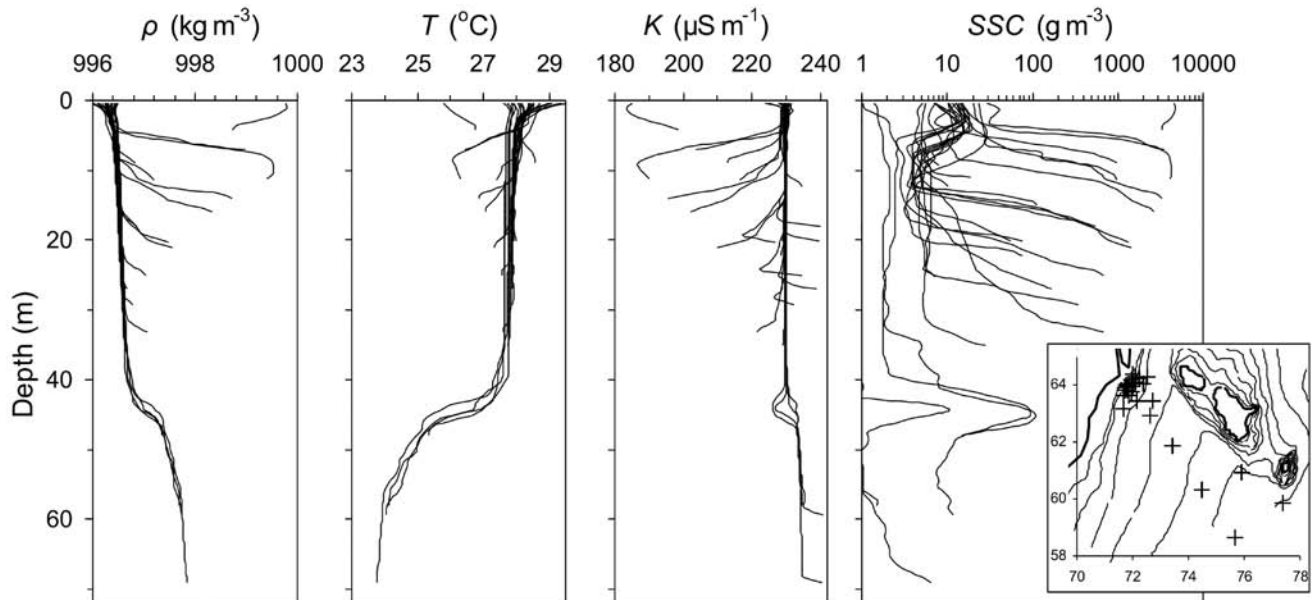


**FIG. 5.** Selected density ( $\rho$ ),  $T$ ,  $K$ , and  $SSC$  profiles recorded SE of the Linthipe River on 17 February 1999. Tails diverging from the general profiles mark layers of relatively dense, cool, dilute and turbid water near the sediment/water interface at the shallower stations. Negative  $K$  and positive  $SSC$  anomalies with peaks at 45 m indicate interflow spreading along the pycnocline/thermocline at the three deepest stations. Profile locations are shown in the map at lower right, where the axes units are UTM coordinates (km) and the isobath interval is 10 m.

bient water column. Moreover, acoustic Doppler current profiles recorded in late January 1999 (McCullough 2006) showed strong downslope currents in such turbid layers.

In almost 90% of profiles recorded between the 10 m and 30 m isobaths SE of the river mouth,  $SSC_{max}$  occurred in the bottom metre of the water column (Fig. 6) and in most of these profiles there was a nearly continuous gradient of increasing  $SSC$  with increasing depth throughout the turbid layer. Where the bottom slope crossed through the metalimnion, underflow separated from the bottom to spread into the lake as interflow. Although some interflow lakeward of the 30 m isobath spread along lesser density gradients in the metalimnion or shallower (Fig. 6) most spread along the highest density gradients near the thermocline. In those profiles lakeward of the intersection of the thermocline with the sediment/water interface, where  $SSC_{max}$  was greater than  $20 \text{ g m}^{-3}$  it typically occurred near the thermocline (within 1 m in 59% of 151 casts CTD casts, and within 3 m in 75% of casts). Where  $SSC_{max}$  did occur below the upper metalimnion, it was usually at the sediment-water interface (points in the lower-right half of the upper-left to lower right diagonal in Fig. 6). These deeper  $SSC_{max}$  at

the sediment-water interface were rarely greater than  $10 \text{ g m}^{-3}$  (Fig. 6), and may in most cases represent bottom nepheloid layers. Concentrations greater than  $20 \text{ g m}^{-3}$  at the surface were also rare; the few higher values in surface plumes were all within a few hundred meters of the shore.

#### Distributions of Mean Concentrations and Load

The above statistics describe only the prevailing conditions through the whole of the rainy season. However, there was considerable sub-seasonal temporal variation in the load and concentration in the delta region. This was particularly so in 1998, when storm runoff was less frequent. Shorter term variation was captured in surveys following a large storm runoff event at the end of February 1998, when a brief, intense flood occurred in the Linthipe River (Fig. 2). Because this storm followed a month of uninterrupted low flow, and because the high flow was marked by low  $K_{LR}$  and high  $SSC_{LR}$  compared to both the pre-existing values in the lake, and to pre- and post-flood values in the river, runoff water and suspended load were clearly distinguishable in the delta region water column in the follow-

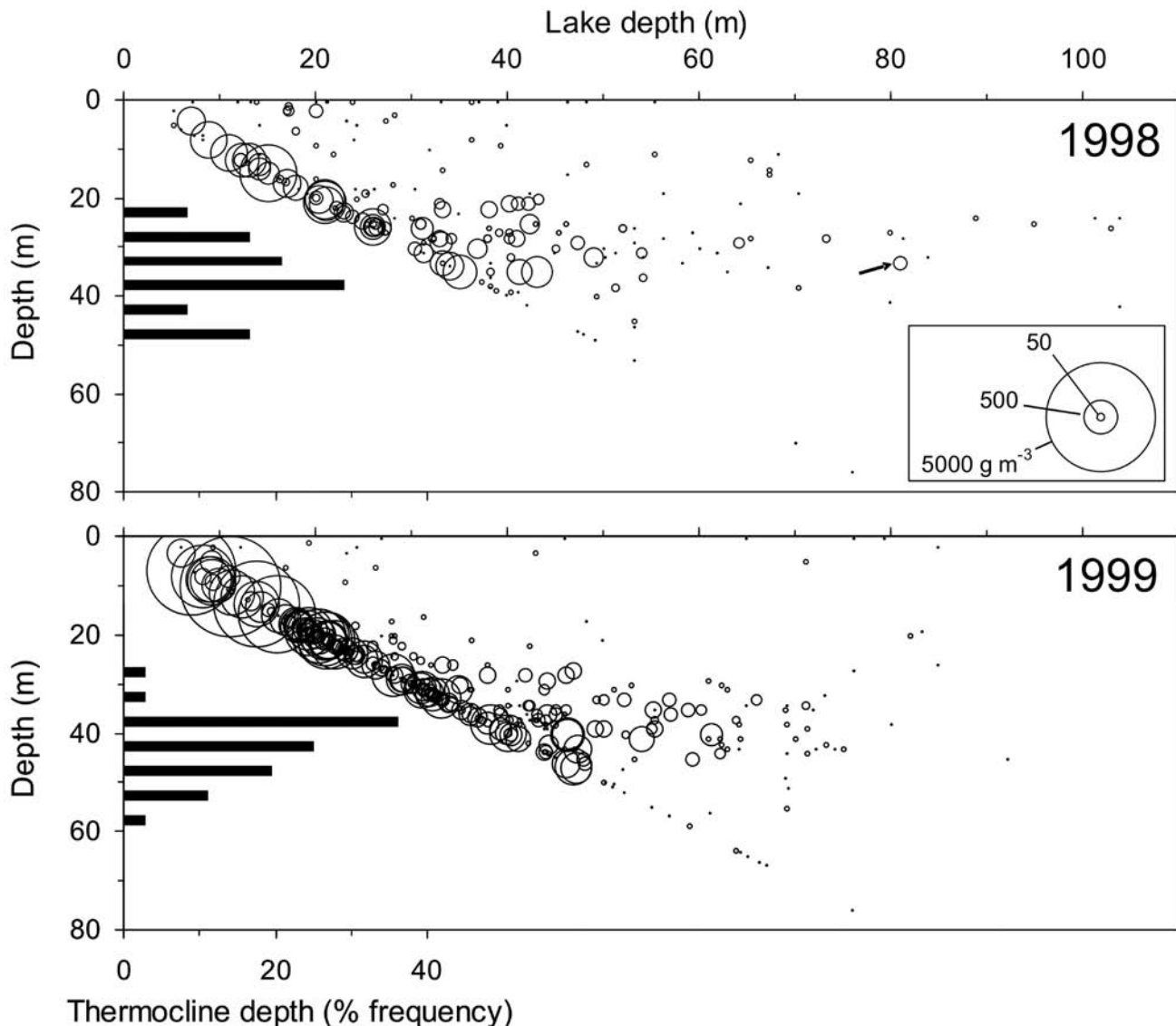


**FIG. 6.** Vertical distributions of  $SSC_{max}$  and histograms of thermocline depth in 1998 (upper panel) and 1999 (lower panel). Depths on the left axis apply to both the bubble plots (depth at which  $SSC_{max}$  was observed) and the histograms (thermocline depth distributions). Values on the upper horizontal axes indicate lake depth. Values on the lower horizontal axes indicate the % frequency of thermocline depths (5 m bins). Legend indicates the area scale of  $SSC_{max}$  in  $g\ m^{-3}$ . (e.g., the circle in the upper panel marked by an arrow represents a cast in 81 m of water in which  $SSC_{max}$  was  $113\ g\ m^{-3}$  and occurred at 33 m depth in the profile. The smallest dots indicate  $SSC_{max}$  of the order of  $1-2\ g\ m^{-3}$ .) Circles falling along the upper-left to lower-right diagonals indicate  $SSC_{max}$  where it occurred at the sediment-water interface; circles falling to the right of this diagonal indicate  $SSC_{max}$  where it was observed in turbid layers separated from the bottom.

ing week. Table 1 shows post-flood distributions of the suspended solids load and mean concentrations in the delta region. Stations used to calculate suspended loads are shown in Figure 7. As in the 17 February 1999 event (Fig. 5), most runoff plunged and flowed downslope until it reached the thermo-

cline, and then spread further into the lake as horizontal interflow largely confined between the mainland on the south and the Maleri Islands ridge on the north. On 1 and 5 March, 90% of the suspended solids load in the water column in a semicircular region within 7 km of the river mouth was in the re-

**TABLE 1.** *Suspended solids load (Gg) and mean concentration (g m<sup>-3</sup>, in parentheses) following storm runoff on 27 and 28 February 1998. Data are shown for 10-m layers in the water column, for 2 semi-circular regions 0–3.5 km and 3.5–7 km from the river mouth. The highest value in each subsample is underlined. Stations used in this determination are shown in Figure 7.*

Depth (m)	Area (km <sup>2</sup> )	Mar 01	Mar 05	Mar 10
<b>0 to 3.5 km</b>				
0–10	22	1.2 (6)	1.3 (6)	1.6 (7)
10–20	17	3.6 (21)	1.7 (10)	1.3 (7)
20–30	12	<u>9.4 (78)</u>	<u>3.0 (25)</u>	<u>1.8 (15)</u>
30–40	5	5.9 ( <u>119</u> )	1.0 (20)	0.3 (6)
40–50	1	0.1 (8)	0.0 (5)	0.1 (5)
Total (Weighted Mean)		20 (36)	7 (12)	5 (9)
<b>3.5 to 7 km</b>				
0–10	65	1.4 (2)	0.6 (1)	1.9 (3)
10–20	58	3.9 (7)	1.2 (2)	1.4 (2)
20–30	48	<u>13.1 (27)</u>	<u>5.3 (11)</u>	<u>2.2 (5)</u>
30–40	42	5.1 (12)	4.1 (10)	0.9 (2)
40–50	29	0.5 (2)	0.4 (1)	0.5 (2)
50–60	14	0.1 (1)	0.1 (1)	0.2 (1)
60–70	7	0.0 (0.3)	0.0 (0.1)	0.0 (1)
Total (Weighted Mean)		24 (9)	12 (4)	7 (3)
<b>0 to 7 km Grand Total</b>		44	19	12

gion S of the Maleri Island chain. This load gradually spread northward, so that by 10 March the distribution (of a considerably smaller total load, 7 Gg on 10 March compared to 24 Gg on 1 March, Table 1) was 70% to the S compared to 30% to the N of the islands.

River discharge peaked on 27 and 28 February 1998 and dropped back to pre-flood level by 4 March (Fig. 2).  $SSC_{LR}$  was as high as 3,270 g m<sup>-3</sup> on 27 February, and remained greater than 1,000 g m<sup>-3</sup> until at least 5 March. Throughout the storm,  $T_{LR}$  was low compared to the 28–29°C of the upper mixed lake water column. The bulk density of river water was calculated to be 998.97 kg m<sup>-3</sup> on 27 February and 997.77 on 1 March, equal to the density of the lake at 280 and 80 m respectively. Nonetheless, the maximum density in underflow was already reduced to < 997 kg m<sup>-3</sup> by the time it crossed the 20 m isobath, that is, to less than the ambient density at 39 m.

Consequently, flow plunged and flowed along the bottom, but attained neutral buoyancy in the metalimnion, where it continued to spread lakeward as interflow. On 1 and 5 March, in a semicircular region within 7 km of the river, three-quarters of the

total load was carried 20–40 m below the surface (Table 1). Less than 10% resided in the upper 10 m of the water column, and only 2–3% was below 40 m depth. By 10 March, the load was more evenly spread through the epilimnion and upper metalimnion—nearly half at 20–40 m depth, but now almost a third in the upper 10 m, with most of the latter in a thin surface plume. On 5 and 10 March, the depth equivalent of the river density was 40 and 31 m respectively. Thus, the density difference between river and lake surface water was much reduced compared to during peak flow, so that in the post-storm period little flow apparently plunged below 30 m. Compared to storm runoff water, more post-storm water spread buoyantly at the surface, accounting for a higher load in the upper 10 m of the water column after more than a week of low flow conditions than in the immediate aftermath of the storm runoff event.

#### Vertical Distributions of SSC in Northern Lake Malawi

In mid-January 1999, water column profiles were recorded along transects near the mouths of the Kiriwa, Songwe, Ruhuhu, and South Rukuru rivers

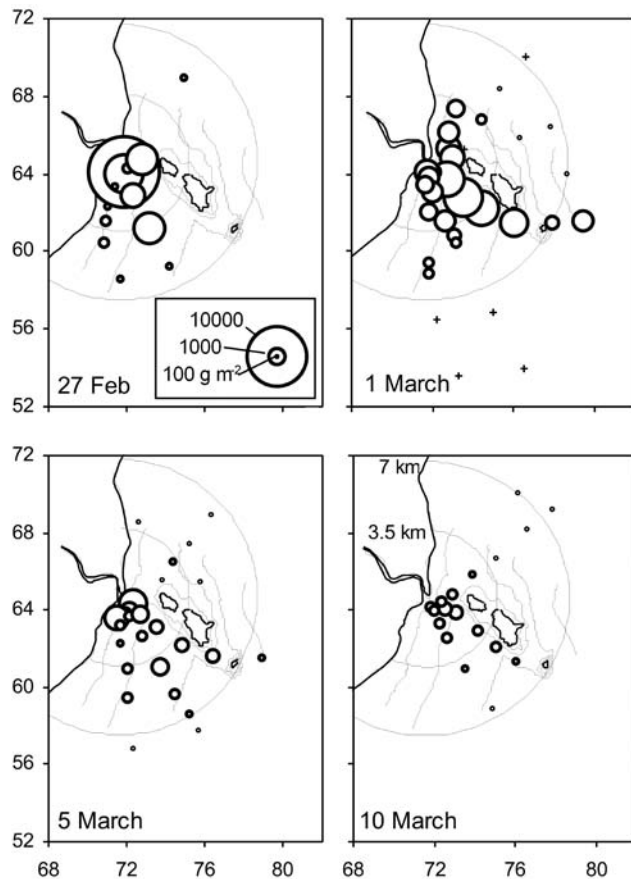


**FIG. 7.** Spatial distribution of suspended solids load (SSL) following 27 February 1998 storm runoff. The two larger concentric circles (marked 3.5 km and 7 km) delineate semi-circular regions for which SSLs is reported in Table 1. Areas of other circles indicate SSL (total through whole water column,  $\text{g m}^{-2}$ ) at the scale shown in the legend. The smallest circles indicate  $\text{SSL} \sim 20 \text{ g m}^{-2}$ ; stations with smaller SSL are indicated by crosses. Bathymetric contour interval is 20 m. Grid is UTM scaled in km.

(Fig. 8) using the same SBE CTD profiler as was used in the Linthipe River delta region. (These casts were made by Harvey Bootsma of the SADC/GEF Lake Malawi/Nyasa Biodiversity Conservation Project, at our request. In addition, Mr. Bootsma allowed us to use his data from five whole-lake survey stations.) In 7 of 18 profiles,  $\text{SSC}$  was less than detection ( $0.01 \text{ g m}^{-3}$ ) throughout (Table 2). In no profile was  $\text{SSC}$  greater than detection at depths greater than 96 m. In 10 of 11 profiles with  $\text{SSC}_{\max} > 0.01 \text{ g m}^{-3}$  the maxima were in the upper metalimnion. In every profile where  $\text{SSC}_{\max}$  was greater

than  $5 \text{ g m}^{-3}$ , it was associated with a high density gradient within 5 m of the thermocline. In the one profile, Rh7, in which  $\text{SSC}_{\max}$  did not lie in the metalimnion, it was a relatively low value ( $\text{SSC}_{\max} = 0.08 \text{ g m}^{-3}$ ) in a thick (18 m) near-surface plume. All but one of the 10  $\text{SSC}_{\max}$  that were recorded in the metalimnion fell within 1 m of  $K_{\min}$ .

## DISCUSSION

In January, 1992, Halfman and Scholz (1993) recorded multiple CTD casts in Lake Malawi near the mouths of each of three large rivers. Near the mouth of the Ruhuhu River (Fig. 1) the upper water column was clear, but a layer of turbid water, with high  $\text{SSC}$  (up to  $30 \text{ g m}^{-3}$ ), depressed  $K$  and elevated dissolved oxygen was observed at 30–65 m depth. They interpreted this to be interflow reaching several kilometers into the lake. They observed smaller  $\text{SSC}$  spikes (up to  $1.5 \text{ g m}^{-3}$ ) in shallower water off the mouths of the Linthipe and Dwangwa rivers, but no similar deep interflow plumes. They speculated that the Ruhuhu produced a deep interflow plume when the others did not either because of intense rains and consequently colder runoff in the Ruhuhu watershed but not in the other watersheds prior to the survey, or because flow through the subaqueous incised valley described by Johnson *et al.* (1995) off the mouth of the Ruhuhu may have allowed the plume to escape shallow redistribution by surface waves and currents.

Our results extend Halfman and Scholz's work by showing that interflow along density gradients near the thermocline is not limited to tributaries with incised subaqueous distributary channels, but is a mechanism that distributes flow from many larger rivers flowing through Lake Malawi. After storm runoff events, peak  $\text{SSC}$  in turbid layers in the upper metalimnion is characteristically more than an order of magnitude higher than in any such layers at shallower depths. In the one post-storm period when we were able to calculate the total load in the water column near the mouth of the Linthipe River, three-quarters of that load resided in plumes at 20–40 m. And turbid plumes more than 5–10 m below the thermocline tend to be weaker and less frequent than those in the upper mixed layer above the thermocline. This was the case not only for the Linthipe River, but also for the Ruhuhu, as Halfman and Scholz's profiles showed, and for several other northern rivers where profiles were recorded in 1999.

In the discussion below 1) we present evidence

**TABLE 2.** Data from surveys near four northern rivers, the Kiwira (Ki), Songwe (So), Ruhuhu (Rh) and South Rukuru (Rk) with watershed areas 1,690, 4,280, 14,070 and 12,110 km<sup>2</sup> respectively. Numbers in parentheses following river names identify CIDA limnological survey stations closest to the rivers in question. The effective instrument range was  $0.01 < \text{SSC} < 40 \text{ g m}^{-3}$ . *K* dilution is the difference between minimum ( $K_{\min}$ ) and *K* at 10 m depth (representative of the ambient upper mixed layer). Among all casts, the range of *K* at 10 m was 230.1–231.0  $\mu\text{S cm}^{-1}$ .

Profile	Time	Distance from river mouth (km)	Depth of CTD cast (m)	Depth of thermocline (m)	<i>T</i> at thermocline (°C)	Depth of $\text{SSC}_{\max}$ (m)	$\text{SSC}_{\max}$ (g m <sup>-3</sup> )	Thickness $\text{SSC} > 5 \text{ g m}^{-3}$ (m)	Deepest SSC > detection (m)	Depth of $K_{\min}$ (m)	<i>K</i> dilution at $K_{\min}$ ( $\mu\text{S cm}^{-1}$ )
Ki1	17 Jan 18:57	0.5	56	31	25.7		< 0.01			17	0.2
Ki2 (927)	17 Jan 17:35	6.6	104	30	26.7		< 0.01			38	0.8
Ki3	17 Jan 18:12	9.0	68	31	26.1	20	0.7		68	19	2.5
So1	17 Jan 16:00	0.3	56	36	26.0	35	6.4	2	56	36	0.8
So2	17 Jan 15:41	1.6	105	31	26.9	36	1.6		96	50	0.7
So3	17 Jan 15:25	3.5	126	38	26.0		< 0.01			37	1.1
So4	17 Jan 14:50	7.2	166	42	25.0		< 0.01			41	1.4
So5 (926)	17 Jan 13:35	18	249	43	25.6		< 0.01			43	1.1
Rh1	19 Jan 14:03	0.5	54	41	25.9	37–40	> 40	13	54	37	33.4
Rh2	19 Jan 13:43	1.9	174	41	25.7	41	6.9	1	43	41	7.7
Rh3	19 Jan 13:04	4.8	192	41	26.1	40	9.4	3	42	40	8.8
Rh4	19 Jan 12:30	7.3	181	36	26.9	40	14.2	3	42	39	7.0
Rh5 (922)	19 Jan 11:12	15	428	26	27.1		< 0.01			40	0.4
Rh6 (923)	19 Jan 07:31	29.5	475	33	27.1		< 0.01			41	0.9
Rh7 (923W)	19 Jan 08:51	30.0	213*	32	27.1	8	0.08		18	39	1.0
Rk1	16 Jan 17:56	0.3	57	31	27.6	28–33	> 40	20	45	31	8.4
Rk2	16 Jan 18:10	1.0	101	29	27.6	27–30	> 40	17	37	28	8.5
Rk3	16 Jan 18:23	1.9	179	32	27.0	29	> 40	6	33	29	9.3

\* Rh7 not recorded to bottom. In other casts, the CTD was lowered to 2–4 m above the sediment-water interface.

that most turbid layers in the epilimnion and metalimnion are of fluvial origin but that the few distinct turbid layers below the metalimnion are more likely to have been developed by resuspension of bottom sediments, and 2) we argue that in current climatic conditions plunging of inflow below the upper metalimnion is probably an infrequent occurrence.

#### Fluvial Origin of Turbid Layers above the Thermocline

There are several potential non-fluvial sources of turbid layers in the epilimnion and metalimnion that may be discounted. Plankton accumulations at the thermocline, either by active buoyancy control or interruption of settling at the density gradient, would have been optically indistinguishable from other suspended solids by our methods. However, plankton accumulations are unlikely to have created

measurable *K* anomalies. On the other hand, several internal physical processes described for Lake Malawi could have caused injection of bottom sediments into the water column at the concentrations that we observed. Johnson *et al.* (1995) present abundant evidence of slope failure and associated turbidity currents in the form of slump scarps and turbidite deposits, particularly in the subaqueous deltas of the northern rivers, although much of this action appears to develop at sub-thermocline depths. They also show sand waves indicating transport by coastal currents, and these tend to be at 30–120 m depths, that is, in the depth range where turbid layers are most frequently observed. These sand waves are more widespread in sub-aqueous deltas on shoaling margins (characterized by relatively shallow offshore slopes) and are particularly

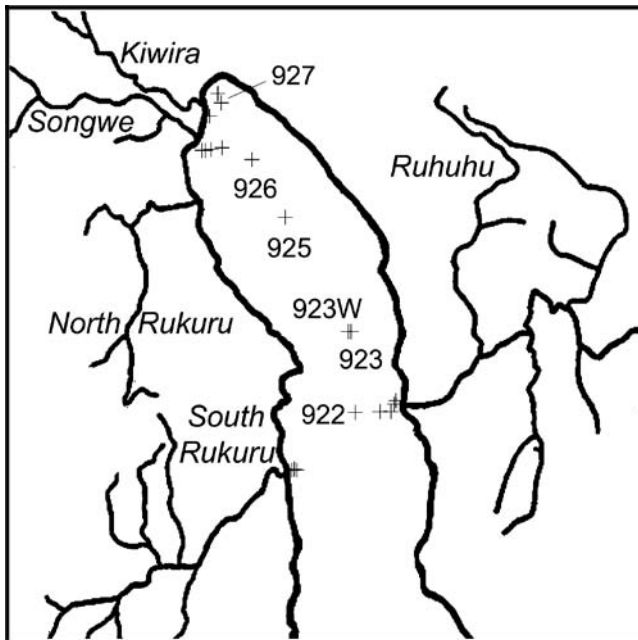


FIG. 8. Locations of CTD casts off the mouths of the Kiwira, Songwe, Ruhuhu, and South Rukuru rivers in January 1999. Numbers identify standard whole lake cruise stations.

common in the sub-aqueous delta of the Linthipe River.

Data from the bottoms of CTD casts show that  $K$  is high in sediment pore water relative to overlying

lake water. In almost two-thirds of casts with the RBR CTD (which was routinely lowered to touch bottom, so that the conductivity sensor frequently penetrated the sediment water interface)  $K$  was 20–40  $\mu\text{S cm}^{-1}$  higher in the deepest observation compared to  $K$  just above the sediment-water interface. Although the magnitude of the difference was not accurately determined, the sign was unambiguously positive and the  $K$  anomaly associated with turbidity generated by resuspension events would be positive if not reduced below detection by dilution.

On the other hand, the  $K$  anomaly associated with Linthipe River water ranged from moderately positive (+ $K$ ) to strongly negative (- $K$ ). Ambient  $K$  was 229–230  $\mu\text{S cm}^{-1}$  in the upper 30 m of Lake Malawi and higher below the thermocline (e.g., 234–236  $\mu\text{S cm}^{-1}$  at 70–80 m depth).  $K_{LR}$  ranged from as low as 130  $\mu\text{S cm}^{-1}$  at the highest flows during which it was recorded, up to 280  $\mu\text{S cm}^{-1}$  at low flow. Because both  $K_{LR}$  and  $T_{LR}$  were inversely correlated with discharge, and  $SSC_{LR}$  was positively correlated (Fig. 3), storm flow tended to be more dense (cooler, with higher  $SSC$ ) than base flow. In fact, rivers are typically characterized by dissolved ion concentrations (hence  $K$ ; see Wüest *et al.* 1996) that are inversely correlated with discharge, and  $SSC$  that is positively correlated (e.g., Leopold *et al.* 1964). Hence, in general we can expect that deep

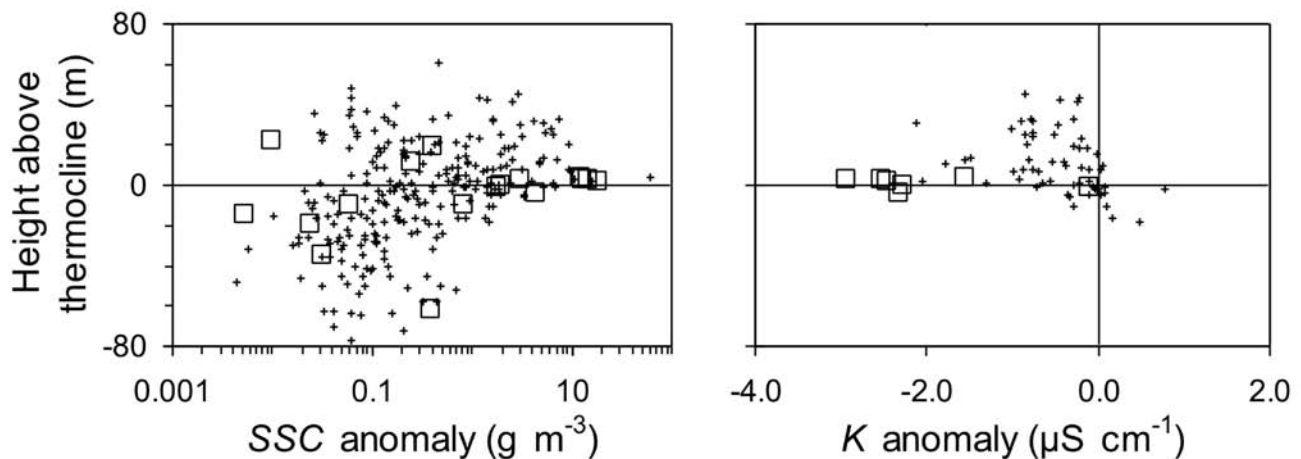


FIG. 9. Mean  $SSC$  and  $K$  anomalies in turbid interflow layers plotted against depth relative to thermocline, in the Linthipe River region (+) and in northern Lake Malawi (□). Turbid layers were identified visually from  $SSC$  profile data. Anomalies are the mean of differences between the actual values and base values calculated by interpolation between values at the top and bottom of each layer.  $K$  anomalies are shown only for layers with  $SSC > 1 \text{ g m}^{-3}$ . Two larger  $K$  anomalies are not shown:  $-10.7$  and  $-6.1 \mu\text{S cm}^{-1}$  at 3 and 4 m above the thermocline respectively, both observed in the Linthipe River region.

turbid layers, if they are of fluvial origin, are likely to be marked by negative  $K$  anomalies in CTD casts. Higher  $K$  base flow, being less dense, is less likely to sink to great depths.

In fact, in Lake Malawi, plumes near or above the thermocline tend to have  $-K$  signals, indicating a fluvial source, and deeper plumes tend to show  $+K$ . Offshore from northern rivers, in layers with  $SSC > 1 \text{ g m}^{-3}$  and  $< 70 \text{ m}$  deep, the  $K$  anomaly was negative. It was positive in the only two deeper  $SSC$  peaks identified in the 16 casts. The tendency to  $-K$  anomalies in turbid layers near or above the thermocline, and  $+K$  anomalies in deeper turbid layers was also observed in the larger sample near the Linthipe River. Figure 9 shows distributions of  $SSC$  and  $K$  anomalies (mean deviations of  $SSC$  and  $K$  in turbid layers or, especially in the case of smaller anomalies, local lenses) relative to the thermocline depth, recorded in the casts near northern rivers and in 82 CTD casts at 70–160 m depth and 7–30 km from the Linthipe River. Large  $SSC$  peaks—with mean  $SSC$  greater than  $10 \text{ g m}^{-3}$ —were always associated with high density gradients just above the thermocline, and were associated with some of the largest  $-K$  anomalies in the deep-water casts. There are three such large  $SSC$  peaks representing a layer of very turbid water resting on the thermocline—at 45 m—in the shallower-water profiles shown in Figure 5. In this case, only the larger two peaks, with  $SSC$  near  $100 \text{ g m}^{-3}$ , are associated with distinct  $-K$  anomalies. In no profiles reaching more than 20 m below the thermocline was the mean  $SSC$  in a local peak greater than  $1 \text{ g m}^{-3}$ . In the deep water casts, in every case in which an  $SSC$  peak near or above the thermocline was associated with a distinct  $K$  anomaly, the latter was negative, indicating a fluvial source (Fig. 9).

#### Improbability of Hyperpycnal Flow Below the Thermocline

However, among the few layers with  $SSC > 1 \text{ g m}^{-3}$  just below the thermocline, none were marked by distinct  $-K$  anomalies; indeed, the largest  $K$  anomalies in this group were positive. Figure 9 shows data only for  $SSC$  peaks in CTD profiles where they were clearly separated from the sediment/water interface. Although there were numerous very small  $SSC$  peaks below the thermocline, none deeper than 20 m below the thermocline had a mean  $SSC > 1 \text{ g m}^{-3}$ . In the deep-water casts near the Linthipe River, there were 40 instances of bottom-attached layers with  $SSC$  peaks  $> 1 \text{ g m}^{-3}$ ; the

$K$  anomaly was distinctly positive in 25 of these, and small or negligible in the rest. The deepest of the profiles shown in Figure 5 has such a bottom-attached layer—13 m thick with a peak  $SSC$  of  $6 \text{ g m}^{-3}$ . For the most part,  $K$  is undiluted in this turbid layer with respect to the overlying water column. (The small positive deviation at the bottom of the profile is caused by a single data point where the sensor may have touched bottom sediments.) Overall, a fluvial source was never positively indicated by distinct  $-K$  anomalies in turbid layers more than a few meters below the thermocline, even though dilute, turbid river water was observed higher in the water column in many of the same profiles.

Kingdon *et al.* (1998) observed that rivers with topographically higher catchments were cooler than rivers, including the Linthipe, with large areas of low-lying lakeshore plains in their catchments. They reported that rainy season mean temperatures of major rivers in the Lake Malawi catchment ranged from 22.3–27.1°C, with the Linthipe River at 26.9°C. They speculated that runoff from cooler, mostly northern rivers would plunge more deeply than flow from warmer southern rivers like the Linthipe. Halfman (1993) speculated that injection of fluvial inputs below the chemocline might occur in exceptionally cold winters but was not likely a frequent occurrence under current climate. In a study of concentrations of the anthropogenic trace gas chlorofluorocarbon-12 in Lake Malawi, Vollmer *et al.* (2002) found that exchange from the upper mixed layer into the monimolimnion occurred predominantly in the southern parts of Lake Malawi. Because deep water fluvial intrusions are expected to be strongest from the colder, northern rivers, they concluded that downwelling of evaporatively-cooled surface water at the south end of the lake is more likely the cause of deep mixing a deep-sinking than is sinking of cool, dense runoff. Vollmer *et al.* (2005) showed that deep injections likely occurred twice in the last 50 y, associated with particularly cold, wet periods, but not more frequently. Our data tend to support Vollmer *et al.*'s contention that deep water fluvial intrusions are rare. In the following paragraphs, we argue that while cooler rivers plunge more frequently to the metalimnion than the Linthipe River, in the current climate they plunge more deeply either rarely or not at all.

McCullough (2006) calculated entrainment of lake water into underflow by analysis of  $K$ -dilution along radial transects of CTD casts, where  $K_{LR}$ , ambient  $K$  in the plunge region, and  $K$  throughout the

underflow layer were all known. Linthipe River water was consistently reduced to about 20% of underflow by the time it intersected the metalimnion. The temperature above the metalimnion was conservatively 28°C in 1998 and 1999. The rainy season mean temperature of the coolest tributary river studied by Kingdon *et al.* (1998) was 22°C. Assuming that the range over the whole rainy season was similar to the Linthipe, 7°C and 8°C through the 1998 and 1999 rainy seasons respectively, then the minimum temperature was 18°C. Given 20% dilution by entrainment of near-surface water, the minimum temperature of the underflow at intersection with the upper metalimnion was 26°C, that is, roughly the temperature at the thermocline, where most dilute, turbid layers were indeed observed in the set of northern CTD casts.

Including the effect of sedimentation does not greatly change the result. In the Linthipe River case, sedimentation removed just under half of the suspended load from underflow within a few hundred meters of the inlet (McCullough 2006). Dilution plus sedimentation would reduce the highest SSC recorded in the Linthipe River, 5,320 g m<sup>-3</sup>, to < 600 g m<sup>-3</sup>, which would add < 0.35 kg m<sup>-3</sup> to bulk density, *i.e.*, the equivalent of lowering the temperature a further 1.3°C beyond the effect of dilution alone. Underflow would reach an equilibrium depth at 24.7°C, roughly 45 m depth or 10 m below the 1999 thermocline, but still well above the ~23.5°C required to sink into the monimolimnion. 50% sedimentation is probably conservative for at least the Ruhuhu and South Rukuru rivers. Both flow into the lake directly off mountain slopes, and are likely to carry a higher proportion of coarse sediments than the Linthipe River, which meanders for almost 30 km through a low-gradient plain before flowing into the lake. In any case, SSC is unusually high in the Linthipe River compared to most runoff into Lake Malawi. Hecky *et al.* (2003) surveyed 13 major tributaries, and found volume-weighted mean SSC to be more than twice as high for the Linthipe River as for all but one of the largest tributaries, the Songwe River. The Linthipe and Songwe are the most densely populated of Lake Malawi's tributary watersheds, with the highest proportions of land cleared for farming. Watersheds with extensive forest cover, even those draining much higher relief landscapes, did not develop nearly as high suspended solids concentrations.

We have assumed that dilution rate for the plunging flow is similar between the northern rivers and the Linthipe. McCullough (2006) used equations

for a buoyant jet (Fischer *et al.* 1979) to show that the dilution measured near the mouth of the Linthipe would have occurred in the initial plunge within 100 m of the mouth. Baines (2005) showed that for flow descending under a stratified fluid along a bottom slope, the probability of jet-like behavior increased with increasing slope. Such jet-like behavior converts to smooth gravity-current-like flow on gentle slopes, where under stratified fluids net entrainment is reduced to near zero (Baines 2005). Johnson *et al.* (1995) showed the slope off the mouths of the South Rukuru and Ruhuhu rivers, which flow into the lake over or close to the border fault margins of sinking half-grabens, to be very steep compared to the slope of the mouth of the Linthipe River, which flows into the lake at the edge of a broad, flat depositional plane overlying the shoaling margin of a similar structure. The initial slopes of the Songwe/Kiwira delta, both of which also cross depositional plains at the lakeshore, are likely similar to the Linthipe, although both drop sharply lakeward of a wide subaqueous shelf (Johnson *et al.* 1995). It is likely, given that underflow from these northern rivers crosses slopes similar to, or steeper than the Linthipe delta slopes, that buoyant jet equations would yield similar results for plunging flow at their mouths.

If so, sedimentation and dilution by entrainment seem to preclude river water plunging much below the thermocline in the current climate, unless a turbidity current develops. Offshore from the Songwe, South Rukuru, and Ruhuhu rivers there are well-defined channels developed by turbidity currents down to 300–450 m (Johnson *et al.* 1995). Sediment-laden water injected from such turbidity currents could be responsible for deep turbid layers like one recorded at 97 m depth, 12 m off the bottom, in profile So2 (1.6 km offshore from the Songwe River) where SSC ranged from 0.04–1.2 g m<sup>-3</sup> through a thickness of 7 m, marked by a small positive *K* signal. (~0.3 μS cm<sup>-1</sup>). However, such channels need not be maintained by currents developed directly from river discharges. Whereas in the Songwe Delta, Johnson *et al.* (1995) showed subaqueous channels beginning at the shallow delta shelf, in the Ruhuhu delta, they observed that the channels originate much deeper, and concluded that they were generated by mass wasting on the mid- and upper slope.

The Songwe River flows more than 1°C colder than the Linthipe River, on average (Kingdon *et al.* 1998) and has a similar volume-weighted mean SSC

(Hecky *et al.* 2003). However, unlike the delta of the Linthipe River, in which a short, steep delta face grades into a long gentle, concave slope, the delta of the Songwe River, beyond a shelf break only 1–2 km from shore, drops steeply to the 100 m isobath (Johnson *et al.* 1995). It and the adjacent Kiwira River are perhaps the most likely of Lake Malawi's tributaries to develop deep-flowing turbidity currents. Downslope channels beginning in relatively shallow water below the river mouth strongly suggest that they do. On the other hand, Johnson *et al.* (1995) reported that the channel floors had a thick veneer of mud, indicating that the latest turbidity flow in the region must have been followed by a period of deposition. One source of such deposition would be sedimentation from a turbid interflow layer such as the one we have described from the January 1999 survey (Table 2). It is likely that both processes occur in the Songwe and Kiwira deltas. In any case, deep turbid layers comprise a very small fraction of the suspended sediment load in Lake Malawi, indicating that development of accelerating turbidity currents which would carry fluvial inputs to great depths may be infrequent relative to hyperpycnal density currents which separate from the bottom and spread as interflow in the metalimnion.

### CONCLUSIONS

The Linthipe River is marked by diurnal temperature fluctuations as great as 5°C and temperature differences between base flow and storm runoff slightly higher. Suspended solids concentrations range to over 5,000 g m<sup>-3</sup> during storm runoff. Over the rainy seasons, temperature contributes 2 kg m<sup>-3</sup> to the density range of the river, more than the density range of the lake, and suspended sediment concentration contributes an additional 2 to 3 kg m<sup>-3</sup>. Dilution and sedimentation reduce density differences between river and ambient lake water within 100s of meters of the river mouth, so that in no case did we observe underflow below the 20 m isobath that was more dense than the lake at 70 m depth. Most underflow separates from the bottom and spreads along the highest density gradients near the thermocline. When we were able to complete a broad survey of the delta region 2 d after a storm runoff event, with the thermocline at 35 m, three-quarters of the suspended load was in thick, turbid layers between 20–40 m depth.

We found similar ionically-dilute, turbid water in the upper metalimnion near every major river sur-

veyed in northern Lake Malawi, as well as at mid-lake stations in both southern and northern Lake Malawi. Although notable surface plumes also developed around river mouths in the aftermath of large runoff events, they were an order of magnitude weaker than interflow in the upper metalimnion. There were few turbid layers much below the thermocline, and these were characterized by positive conductance anomalies, suggesting resuspension of bottom sediments. We argue that—except by the action of turbidity currents—runoff must rarely sink below the upper metalimnion. The upper metalimnion is the prevailing pathway carrying watershed runoff and suspended solids horizontally throughout Lake Malawi.

### ACKNOWLEDGMENTS

We thank the Government of Malawi for permission to carry out this research and for discharge data for the Linthipe River. The project was funded by the Canadian International Development Agency (CIDA) with logistical support from the Southern African Development Community/Global Environmental Facility's Lake Malawi/Nyasa/Niassa Biodiversity Conservation Project. It benefited from additional financial support through Natural Sciences and Engineering Research Council of Canada and Canada Research Chair grants to D. Barber. At our request, Harvey Bootsma of CIDA kindly recorded CTD profiles off the mouths of several northern rivers. We would particularly like to thank the late Elias Mnenula, who capably manned our survey boat on Lake Malawi.

### REFERENCES

- Amin, M.A., and Barton, D.R. 2003. Environmental factors controlling the distributions of benthic invertebrates on rocky shores of Lake Malawi, Africa. *J. Great Lakes Res.* 29 (Supplement 2):202–215.
- Baines, P.G. 2005. Mixing regimes for the flow of dense fluid down slopes into stratified environments. *J. Fluid Mech.* 538:245–267
- Bootsma, H.A., and Hecky, R.E. 1993. Conservation of the African Great Lakes: a limnological perspective. *Conservation Biology* 7(3):644–656.
- Chen, C.F., and Millero, F.J. 1986. Precise thermodynamic properties for natural waters covering only the limnological range. *Limnol. Oceanogr.* 31:657–662.
- Cooley, P.M. 2004. The Coastal Habitats, Species Composition, Richness, and Temporal Variation of Haplochromine Cichlids in an African Great Lake: implications for biodiversity conservation. Ph.D. thesis. University of Manitoba, Winnipeg, Canada.

- DOW. (Department of Water, Malawi and United Nations Dept. of Tech. Cooperation for Development). 1986. *Republic of Malawi National Water Resources Master Plan, Annex 4*. UNDP Projects MLW-79-015/MLW-84-003.
- Duponchelle, F., Ribbink, A.J., Msukwa, A., Mafuka, J., and Mandere, D. 2000. The potential influence of fluvial sediments on rock dwelling fish communities. Chapter 6. In *Fish Ecology Report, Lake Malawi/Nyasa/Niassa Biodiversity Conservation Project*, Duponchelle, F. and Ribbink, A., eds., pp. 227–264.
- Fischer, H.B., List, E.J., Koh, R.C., Imberger, J., and Brooks, N.H. 1979. *Mixing in Inland and Coastal Waters*. New York: Academic Press, Inc.
- Gonfiantini, R., Zuppi, G.M., Eccles, D.H., and Ferro, W. 1979. Isotope investigations of Lake Malawi. In *Isotopes in lake studies*, pp. 192–205. (Proceedings of International Atomic Energy Agency conference on the application of nuclear techniques to study of lake dynamics, Vienna, 1977.) IAEA Panel Proceedings Series STI/PUB/511.
- Guildford, S.J., Taylor, W.D., Bootsma, H.A., Hendzel, L.L., Hecky, R.E., and Barlow-Busch, L. 1998. Factors controlling pelagic algal abundance and composition in Lake Malawi/Nyasa. In *Water Quality Report: Lake Malawi/Nyasa Biodiversity Conservation Project*, H.A. Bootsma and R.E. Hecky, eds. SADC/GEF Lake Malawi/Nyasa Biodiversity Conservation Project.
- Halfman, J.D. 1993. Water column characteristics from modern CTD data, Lake Malawi Africa. *J. Great Lakes Res.* 19:512–520.
- , and Scholz, C.A. 1993. Suspended sediments in Lake Malawi, Africa: a reconnaissance study. *J. Great Lakes Res.* 19:499–511.
- Hecky, R.E., Bootsma, H.A., Mugidde R.M., and Bugenyi, F.W.B. 1996. Phosphorous pumps, nitrogen sinks, and silicon drains: Plumbing nutrients in the African Great Lakes. In *The Limnology, Climatology and Paleoclimatology of the East African Lakes*, 1st ed. T.C. Johnson and E.O. Odada, eds., pp. 205–224. Gordon and Breach Publ., Amsterdam.
- , Bootsma, H.A., and Kingdon, M.L. 2003. Impact of land use on sediment and nutrient yields to Lake Malawi/Nyasa (Africa). *J. Great Lakes Res.* 29(Supplement 2):139–158.
- Johnson, C.J., Wells, J.D., and Scholz, C.A. 1995. Deltaic sedimentation in a modern rift lake. *Geol. Soc. of America Bull.* 107(7):812–829.
- Kidd, C.H.R. 1983. *A Water Resources Evaluation of Lake Malawi and the Shire River*. UNDP Project MLW/77/012, World Meteorological Organization, Geneva.
- Kingdon, M.J., Bootsma, H.A., Mwita, J., Mwichande, B., and Hecky, R.E. 1998. River discharge and water quality. In *Water Quality Report: Lake Malawi/Nyasa Biodiversity Conservation Project*, H.A. Bootsma and R.E. Hecky, eds. SADC/GEF Lake Malawi/Nyasa Biodiversity Conservation Project.
- Lambert A.M., Kelts K.R., and Marshall N.F. 1976. Measurements of density underflows from Walensee, Switzerland. *Sedimentology* 23:87–105
- Leopold, L.B., Wolman, M.G., and Miller, J.P. 1964. *Fluvial Processes in Geomorphology*. W.H. Freeman and Co., San Francisco, U.S.A.
- McCullough, G.K. 2006. Circulation of Terrestrial Runoff and its Suspended Load in a Large Tropical Lake. Ph.D. thesis, University of Manitoba.
- , and Barber, D.G. 2007. The effect of suspended solids loading from the Linthipe River on light in Lake Malawi. *J. Great Lakes Res.* 33:466–482.
- Patterson, G., and Kachinjika, O. 1995. Limnology and phytoplankton ecology. In *The Fishery Potential and Productivity of the Pelagic Zone of Lake Malawi/Niassa*, A. Menz, ed. Natural Resources Institute, Chatham, U.K.
- Spigel, R.H., and Coulter, G.W. 1996. Comparison of hydrology and physical limnology of the East African Great Lakes: Tanganyika, Malawi, Victoria, Kivu and Turkana (with reference to some North American Great Lakes). In *The Limnology, Climatology and Paleoclimatology of the East African Lakes*, 1st ed. Thomas C. Johnson and Eric O. Odada, eds., pp. 103–138. Amsterdam: Gordon and Breach Publishers
- Sululu, R.S.M. 2000. Impact Of Suspended Sediments On The Abundance And Species Richness Of The Sandy-Shore Dwelling Haplochromine Cichlids In Southwestern Lake Malawi / Nyassa (East Africa). M.Sc. thesis, U. of Waterloo, Waterloo, Canada.
- Vollmer, M.K., Weiss, R.F., and Bootsma, H.A. 2002. Ventilation of Lake Malawi/Nyasa. In *The East African Great Lakes: Limnology, Paleolimnology and Biodiversity: Advances in Global Change Research*, E.O. Odada and D.O. Olago, eds., pp. 209–233. Kluwer Publishers, Dordrecht, 209–233, 2000.
- , Bootsma, H.A., Hecky, R.E., Patterson, G., Halfman, J.D., Edmond, J.M., Eccles, D.H., and Weiss, R.F. 2005. Deep-water warming trend in Lake Malawi, East Africa. *Limnol. Oceanogr.* 50(2): 727–732.
- Wüest, A., Imboden, D.M., and Schurter, M. 1988. Origin and size of hypolimnic mixing in Urnersee, the southern basin of Vierwaldstättersee (Lake Lucerne). *Schweiz. Z. Hydrol.* 50:40–70.
- , Piepke, G., and Halfman, J. D. 1996. Combined Effects of Dissolved Solids and Temperature on the Density Stratification of Lake Malawi. In *The Limnology, Climatology and Paleoclimatology of the East African Lakes*. 1st ed. T.C. Johnson and E.O. Odada, eds., pp. 183–202. Amsterdam: Gordon and Breach Publ.

Submitted: 27 October 2005

Accepted: 31 January 2007

Editorial handling: Ram R. Yerubandi